

# The Enrichment History of Hot Gas in Poor Galaxy Groups

David S. Davis

Center for Space Research NE80-6003, Massachusetts Institute of Technology, 77 Massachusetts Ave, Cambridge, MA 02139-4307

John S. Mulchaey

The Observatories of the Carnegie Institution of Washington, 813 Santa Barbara St., Pasadena CA 91101-1292

and

Richard F. Mushotzky

Laboratory for High Energy Astrophysics, NASA/GSFC, Code 662, Greenbelt, MD 20771

## ABSTRACT

We have analyzed the ASCA SIS and GIS data for seventeen groups and determined the average temperature and abundance of the hot x-ray emitting gas. For groups with gas temperatures less than 1.5 keV we find that the abundance is correlated with the gas temperature and luminosity. We have also determined the abundance of the  $\alpha$ -elements and iron independently for those groups with sufficient counts. We find that for the cool groups (i.e.  $kT < 1.5$  keV) the ratio of  $\alpha$ -elements to iron is  $\sim 1$ , about half that seen in clusters. Spectral fits with the S, Si and Fe abundances allowed to vary separately suggest the S/Fe ratio is similar to that seen in clusters while the Si/Fe ratio in groups is half the value determined for richer systems. The mass of metals per unit blue luminosity drops rapidly in groups as the temperature drops. There are two possible explanations for this decrease. One is that the star formation in groups is very different from that in rich clusters. The other explanation is that groups lose much of their enriched material via winds during the early evolution of ellipticals. If the latter is true, we find that poor groups will have contributed significantly (roughly 1/3 of the metals) to the enrichment of the intergalactic medium.

*Subject headings:* interstellar medium - X-rays: galaxies - galaxies: intergalactic medium - cosmology: dark matter

## 1. Introduction

Poor groups of galaxies are the most common aggregation of galaxies known and thus are the likely repository of much of the material in the low redshift universe (cf Fukugita, Hogan and Peebles 1998). In a hierarchical clustering scenario for the growth of structure in the universe they are the first steps in the growth of large scale structure. These systems provide a unique opportunity to study the processes which may occur in more massive systems, such as rich clusters, but with much less complexity. X-ray data for poor groups allow the investigation of the enrichment and heating of the intra-group medium, mass profiles of poor systems, and the global properties of low mass systems. Because these groups are the most common structure in the universe their properties should reflect the processes that dominate the production and ejection of metals for most stellar systems. In this study we focus on the enrichment history of the group gas.

Early hints that some groups might contain diffuse gas were provided by the Einstein Observatory (Biermann, Kronberg & Madore 1982; Bahcall, Harris & Rood 1984); but, the Einstein IPC could not clearly distinguish the x-ray emission from the galaxies and the more diffuse emission of the group. The *ROSAT* PSPC is better suited to the search for cool diffuse gas associated with groups. With superior spatial resolution, sensitivity to less energetic x-rays, wider field of view and lower internal background than the Einstein IPC, *ROSAT* has provided a large sample of groups with diffuse x-ray gas (Henry et al. 1995, Pildis, Bregman, & Evrard 1995, Mulchaey et al. 1996, Ponman et al. 1996). These data demonstrate that extended x-ray emission from groups is a

rather common property of these systems. The implied dark matter distribution often extends on scales much larger than that inferred from the distribution of the bright galaxies in these groups. In many groups, the x-ray emitting gas is a major fraction of the total baryonic mass.

While the *ROSAT* PSPC is well suited for detecting the low surface brightness diffuse group gas, its most obvious shortcoming is the lack of spectral resolution. However, the PSPC is quite sensitive around  $\sim 1$  keV, just where the iron L complex can dominate the x-ray emission for cool systems and, in principle, should be able to measure the iron abundance in these systems. Some questions have been raised about the accuracy of the PSPC abundance determinations (Bauer & Bregman 1997). Because the PSPC does lump all the emission from the iron L region into one spectral feature these concerns may be warranted. With its superior spectral resolution, wider energy band, and modest spatial resolution, the x-ray telescope ASCA can be used to better constrain the temperature and abundance of the hot extended gas. In particular, the ASCA SIS data can resolve lines and line complexes from various elements in the spectra from the diffuse gas. Direct comparison of the ASCA and PSPC abundance measurements have the potential for verifying the accuracy of the much larger PSPC data base.

## 2. Observations and Spectral Fits

The groups analyzed here are from our accepted ASCA program and from the public data archive and therefore, do not form a complete sample. Table 1 shows the ASCA group data presented in this paper. The table

lists the group name in column 1, followed by the Right Ascension and Declination in the next two columns. Columns 4 and 5 list the heliocentric radial velocity and the velocity dispersion of the group. The final column of the table lists the total blue luminosity of the galaxies in the group, with the total blue magnitude taken from the RC3 when available. Otherwise, the magnitude is taken from the original source (e.g. Hickson et al. 1989; Zabludoff & Mulchaey 1998).

Prior to extracting the group spectra the ASCA data are screened using the default criteria to eliminate periods of high background, SAA passage and earth block. Background spectra for the SIS and GIS are from the files generated from blank sky data and are subtracted from the source spectra. In a few cases, the group emission did not fill the GIS FOV. For these groups we used a local background for determining the source spectra. The spectra for the global fits were extracted from the center of the group to the edge of the group emission as observed by the *ROSAT* PSPC data. When no PSPC data were available for the groups we estimate the extent from the smoothed GIS data.

In the cases where we detected x-ray emission from other sources in the field we excluded a circular region  $3'$  in radius around the source. This does not remove all the contaminating flux from the extracted spectra. However, given the observed count rates of the contaminating point sources in these fields, we expect only a handful of “contaminating” counts in the resulting group spectrum. We did not exclude the central elliptical galaxy from the group gas spectrum.

The extracted spectra are grouped so that

they have a minimum of 25 counts per channel. The grouped spectra are fit using XSPEC 9.0 with a Raymond-Smith plasma model with an absorbing column. We fixed the  $N_H$  to the Galactic value for one set of fits and repeated the fit with  $N_H$  free to vary. In general, this did not affect the fitted parameters significantly except to increase the error estimates in the variable  $N_H$  case. In addition to the spectral fits with the abundance of the individual elements in the model varying together, for some spectra we also allowed groups of elements to vary independently using the VRAYMOND model in XSPEC.

We fit the SIS and GIS data jointly to determine the temperature and abundance of the group gas. The results are listed in table 2 and are emission weighted values for the group. Temperature or metallicity gradients in the groups will complicate the discussion. The errors given in table 2 are the 90% confidence errors. The Galactic  $N_H$  values are from Dickey & Lockman (1990). To assure that the x-ray properties of the groups listed in table 2 are uniform we have re-analyzed the data for several groups that also appear in the literature. For example, the ASCA data for NGC 5044 and HCG 51 have been analyzed by Fukazawa et al. (1996). Our temperatures and abundances agree with their determinations within the 90% confidence errors. In addition to those we have HCG 62, MKW4s, and MKW9 in common with the groups analyzed by Hwang (1997) and again our derived temperature and abundance agrees very well with her results. So, unlike the case with the *ROSAT* PSPC analysis for groups which showed wide variations of x-ray properties depending on the analysis method, the ASCA results seem to be fairly robust. We will compare the ASCA and *ROSAT* PSPC results

in more detail in a later paper (Mulchaey et al. 1998), but in general we find good agreement between the ASCA and *ROSAT* results.

### 3. Diffuse Gas in Groups

The gas temperature in equilibrium systems reflects the depth of the potential well. The majority of groups in our sample show a fairly narrow range of temperature. The group temperatures peak at around 1 keV which is consistent with the narrow range of masses for poor groups found by Mulchaey et al. (1996). The x-ray temperature of the NGC 3258, NGC 4104 and MKW 9 groups are about twice the characteristic temperature of the cooler groups which indicates that these are more massive systems. The seventeen groups span a much larger range in metal abundance (from  $<0.05$  solar to 0.55 solar with a median value of 0.25 solar). The three groups that we identify as “hot” do not distinguish themselves in metal abundance with all three having abundances close to the median value.

The metal abundance in these groups appears to show a strong variation with temperature (figure 1), in the sense of increasing metal abundance with increasing temperature for temperatures below about 1.5 keV. This is very different from the trend seen in richer systems. The metal abundance for clusters of galaxies shows either no variation (Fukazawa et al. 1996) or a slow rise in the metal abundance between 10 – 2 keV (Arnaud et al 1992; Hatsukade 1989). With the addition of groups it is clear that below a temperature of  $\sim 1.5$  keV the measured Fe abundance drops quickly to about half the value seen in the hotter groups and continues to drop for the lower temperature

systems. A correlation between the temperature and abundance seems to be present in the data (see figure 1). Using Kendall’s  $\tau$  to test for the presence of a correlation, we find less than a 3% chance that a correlation is not present in the data. Fitting the data with a power law, we find that the best fit power law is Abundance  $\propto kT(\text{keV})^{+2.5 \pm 0.94}$ , which is quite different from that found for clusters (Abundance  $\propto kT(\text{keV})^{-0.37}$ ; Arnaud et al. 1992). Unlike clusters, there is no clear correlation between the mass of Fe in the ICM vs  $L_B$  (Arnaud et al 1992). The correlation between abundance and x-ray luminosity is stronger but we defer that analysis to Mulchaey et al. (1998) where we will use the more accurate *ROSAT* PSPC fluxes.

To determine the relative abundance of elements other than Fe we fit the x-ray spectra with a Raymond-Smith plasma model with variable abundances (VRAYMOND). For these fits O, Ne, Mg, Si, and S (the  $\alpha$ -elements;  $A_\alpha$ ) vary together. Fe and Ni vary in unison, and He, C, N, Ca, Ar are fixed at the solar value. The ten groups with sufficient signal-to-noise to determine the abundance of iron and the  $\alpha$ -elements separately are listed in table 3a. All the groups in table 3a are well fit with the VRAYMOND model with the exception of the NGC 5044 group. For NGC 5044 the group gas shows a strong metallicity gradient and cannot be characterized by a global abundance. It will be discussed in a later paper.

Most of the groups listed in table 3a have the abundance of the  $\alpha$ -elements equal to the abundance of iron (within the errors). The only two exceptions are the N4104 group and MKW9, which have the iron abundance about half that of the  $\alpha$ -elements. To quantify this, the average of the  $\alpha$ -elements and the average

of the iron abundance  $\langle A_\alpha \rangle / \langle A_{Fe} \rangle$  is 1.22, but if we exclude the “hot” groups ( $kT > 1.5$ ) then the average ratio drops to 0.96. For the two hot groups (NGC 4104 and MKW 9) the average  $\langle A_\alpha \rangle / \langle A_{Fe} \rangle$  is 2.1.

The spectral resolution of the SIS allows us to fit some of the individual line complexes. For the groups with greater than  $\sim 10000$  counts in the SIS data we allowed O, Si, S, and Fe to vary independently. The results of the fits are shown in table 3b. These global fits will include emission from any hot gas from the central elliptical which might be distinct from the group gas. The oxygen abundance is not well constrained for any of the groups examined here, so the large range in the O/Fe ratio (from a high of 6 to a low of 0.5) may not be particularly meaningful. The S/Fe ratio is fairly constant ranging from 1.4 – 0.9 and is, on average, slightly larger than that seen in clusters  $\sim 0.78$ . The Si/Fe ratio in groups varies from 2.7 – 0.8 with the ratio of Si to Fe in the hot groups at the high end and the cool groups at the low end. Clusters show an average Si/Fe ratio of  $\sim 2$  (Mushotzky et al. 1996). Thus, the average for the groups (Si/Fe  $\sim 1.1$ ) is significantly lower than that of clusters. This trend for the silicon to iron ratio to increase as the temperature (i.e. mass) of the system increases has previously been noted by Fukazawa et al. (1996).

## 4. Discussion

The detection of hot x-ray gas in galaxy groups has opened a window into the history of the x-ray emitting gas in galaxy systems of mass  $\sim 10^{13}$ – $10^{14} M_\odot$ . The ASCA data allow us to directly probe the elemental abundance of the hot gas. With this information we can begin to

answer some of the questions about the origin of heavy elements in groups and poor clusters. Among the issues that need to be resolved are the variation of abundance with temperature, the origin of the metals, and why groups appear to have different enrichment histories than rich clusters.

### 4.1. Supernovae in Enrichment of the Diffuse Gas

The enrichment of the hot gas seen in groups and clusters of galaxies is widely believed to be from processed stellar material transported out and mixed with the hot gas in the system. The favored models contain a large number of type I and type II SNe early in the lifetime of the cluster, when elliptical galaxies are forming stars at a rapid rate (Renzini et al. 1993). Since type I SNe will produce mostly iron and type II SNe will produce the  $\alpha$ -process elements in addition to iron, high resolution x-ray spectroscopy can, in principle, be used to determine the relative rate of type I and type II SNe over the enrichment history of the diffuse hot gas. However, the amount of iron produced in type II SN events is uncertain (Loewenstein & Mushotzky 1996). The ratio of  $A_\alpha$  to  $A_{Fe}$  measured in clusters,  $\sim 2$ , favors the majority of the metals originating from type II SNe ejecta (Mushotzky et al. 1996; Loewenstein & Mushotzky 1996). In our group sample, the ratio of  $A_\alpha$  to  $A_{Fe}$  is  $\sim 1$ , implying that type II SNe are less prevalent in the early evolution of groups than in rich clusters.

However, interpreting this ratio is further complicated by the possibility of multiple star formation events in the galaxy. If the early wind phase of the galaxy is predominately

powered by type II SNe and later star formation episodes are dominated more and more by type I SNe then the detailed star formation history of the system is needed to interpret the ratio of  $A_\alpha$  to  $A_{Fe}$  with confidence. If we take the metal abundances at face value then the relative abundance of the  $\alpha$ -process elements to iron indicates that for groups both type I *and* type II SNe contribute significantly to the enrichment of the diffuse gas. This is in contrast to clusters where type II SNe seem to dominate the enrichment of the diffuse gas (Mushotzky et al 1996, but see Gibson, Loewenstein and Mushotzky 1997 for a discussion of the wide range of possibilities).

The ratio of  $\alpha$ -elements to iron is very sensitive to the supernova model used in the calculation. The expected abundances relative to iron for various supernova models have been tabulated by Loewenstein & Mushotzky (1996)(table 4). The data for the hot groups show that the Si/Fe ratio is  $\sim 2.5$  while for the cooler groups it is  $\sim 1$ . This, along with the average S/Fe ratio of  $\sim 0.78$ , indicates that the Woosley & Weaver (1995) models with zero abundances (WW0) and models with zero abundances and enhanced SNe for  $M > 25 M_\odot$  (WW0e) fit the observed ratios best. None of the models they tabulate fit the high O/Fe ratio seen in the NGC 4104 group, but the oxygen abundance is not well-constrained by the ASCA data. The low O/Fe ratio seen in the cool groups, if confirmed, would be consistent with the zero abundance models.

The mass to light ratio of various elements is a powerful tool for determining the type of SNe events which have enriched the hot gas in groups and clusters (Renzini et al. 1993). The mass to light ratio for O, Si, and Fe using

various SNe models has been tabulated by Loewenstein & Mushotzky(1996) to determine the best scenarios for the enrichment of the hot gas in clusters. Here we examine the mass to light ratios of the groups in our sample to determine the enrichment history of groups.

The element that is best determined in these x-ray spectra is iron. The  $M_{Fe}/L_B$  for the groups ranges from  $(0.5 - 54.5) \times 10^{-5}$  in solar units (table 4). This is much lower than the typical cluster value of  $\sim 0.02 M_\odot/L_\odot$ . Examining table 3a of Loewenstein & Mushotzky 1996, we find that only the models with very steep IMF ( $x=2.35$ ) can fit the observed data. But because type I and type II SNe can eject iron into the ISM, this element is not well suited for determining the type of early SNe events that enrich the hot gas. We have determined the mass to light ratio for individual  $\alpha$ -elements in four groups. The oxygen mass to light ratios range from  $(2.4 - 21.8) \times 10^{-3} M_\odot/L_\odot$  while the silicon mass to blue light ratio is between  $(3.7 - 18.2) \times 10^{-4} M_\odot/L_\odot$ . The O/ $L_B$  and Si/ $L_B$  ratios are consistent with IMF's with a slope steeper than about  $x = 1.8$ . But when we include the  $M_{Fe}/L_B$  ratios only the models with zero initial stellar abundance and enhanced SNe rate can reproduce the elemental mass to light ratios in these groups.

## 4.2. Mass Loss from Galaxy Groups

The ASCA data show that groups have less metals in their hot gas than do clusters per unit blue light. This low metal mass to light ratio is due both to a low overall abundance and to a relatively lower hot gas to total mass ratio. The low ratio seen in the groups could

be the result of several different processes. One could be that the metal production per unit light may vary with environment e.g. with local density. A second possibility is that groups lose large amounts of metals during their evolution (White 1991; David et al. 1990; David et al. 1991; Renzini 1997). We examine both of these scenarios below.

If environment is the key then there must be a feedback process between the conversion of gas into stars and the large scale environment. Such an effect is indicated by the morphology density relation (Dressler 1980). Because the rich clusters are much larger density perturbations than the poor groups such a process might be related to a greater efficiency of star production from gas in overdense perturbations that will become the rich clusters. However, there is no indication of any difference in the stellar populations of ellipticals that reside in clusters or in the poor groups. Because the total light of the groups is dominated by spheroidal systems one suspects that the metal production rate is also dominated by spheroidals. Thus, if local density is the controlling factor then the conversion of gas into stars and therefore into metals must somehow have produced "normal" stellar populations. This local process must also result in a lower metal to blue light ratio than for similar stellar populations in rich clusters.

The proposition that groups lose most of their enriched gas is consistent with models (Arnaud et al. 1992; Renzini et al. 1993) in which the production of metals creates enough energy to produce a large scale wind. The additional average energy per particle produced by metal formation is roughly equivalent to the binding energy of the groups (Loewenstein and Mushotzky 1996). Thus the ejection of metals

from groups is not unexpected. Additionally, if groups form from smaller subunits and if the infall velocity is thermalized this can provide sufficient energy to eject the IGM (Gnedin & Ostriker 1997).

Further evidence in support of the wind hypothesis comes from the metal mass to light ratios. Because clusters and groups of galaxies are not closed systems and can exchange gas with the surrounding environment (Ciotti et al. 1991 and the above discussion), the ratio of mass of metals in the gas to the total blue luminosity of the galaxies is a more useful quantity for determining the enrichment history of the gas (Renzini et al. 1993) than the relative abundances of the individual elements.

For a large data base of clusters, Arnaud et al. (1992) found that in the ICM the  $M_{Fe}$  was proportional to the total blue luminosity, and that the trend was for cooler clusters to have a higher abundance. However, this trend is rather shallow and Renzini et al (1993) adopted a typical value of  $M_{Fe}/L_B = 0.01 - 0.02 M_{\odot}/L_{\odot}$ . For groups the "typical" value of  $M_{Fe}/L_B$  is  $\sim 0.0001$  but as can be seen in figure 2 the value of  $M_{Fe}/L_B$  drops rapidly as the group temperature drops. Therefore, it is likely that the groups must lose most of the enriched gas that the galaxies in the group can produce (see the discussion above). This also indicates that for hierarchical clustering the poor groups we see today cannot be the building blocks of the richer systems unless the ejected gas is globally bound to a collection of merging systems.

The global enrichment of hot group gas varies with temperature in the opposite sense than is seen in clusters; in clusters the metal abundance increases with decreasing temperature. For groups with temperatures less

than 1.5–2 keV the trend is increasing metal abundance with increasing temperature. Figure 1 shows the group data along with a solid line showing the trend for clusters (Arnaud et al. 1992). The break from the abundance predicted from clusters at  $\sim 1.5$  keV is consistent with the lower mass systems losing part of the metal rich gas ejected from the galaxies (Mulchaey et al. 1993; Renzini et al. 1993; Davis et al. 1996). If current models of elliptical evolution are correct then the least massive (coolest systems) must lose most of their processed material.

The observation that in clusters the  $M_{Fe}/L_B$  is fairly constant is an indication that massive clusters are probably closed systems and have not lost or accreted metals from outside the cluster; or, if they have done so the process must have a very narrow range of allowed variance. However, the fact that the average cluster abundance does show variations (Scharf & Mushotzky 1997) indicates that there is true variation from object to object. If clusters were losing mass via winds (or some such mechanism) then the less massive (cooler) systems would lose more gas and the  $M_{Fe}/L_B$  would be smaller for cooler systems. Similarly, if clusters were accreting primordial gas from outside the cluster then the clusters accreting the most gas (the most massive systems) would have their metals diluted more, resulting in a trend in  $M_{Fe}/L_B$ . Since only a mild trend is observed in clusters it is assumed that clusters are closed systems. The simplest high density hierarchical models form clusters at low redshift from the merger of groups. This is not consistent with our data since the cluster properties would be the average of the group properties and our results show that the average group has lower  $M_{Fe}/L_B$ , lower metal abundance and a lower gas mass fraction than the rich clusters.

However, more complex models in which the timescale for metal production, the collapse of high density perturbations, and the possibility of a low density universe are included, can be made consistent with our results.

For groups, strong downward trends are seen in the  $M_{Fe}/L_B$  data. Because groups of galaxies show a strong trend of decreasing abundance with decreasing temperature (mass) then using the arguments above it seems that groups of galaxies show evidence for mass loss from winds. So, unlike clusters, groups are not closed systems. While mass loss from groups can explain the decreasing trend seen in the  $M_{Fe}/L_B$  ratio there could be other explanations. One possible method of altering the  $M_{Fe}/L_B$  ratio between systems is to change the initial mass function. The consistency of  $M_{Fe}/L_B$  in clusters indicates that the initial mass function (IMF) does not change much from cluster to cluster (Renzini et al. 1997; Wyse 1998). To adjust the IMF for groups only to explain the  $M_{Fe}/L_B$  ratio seems rather contrived given the lack of evidence and we don’t consider this a likely explanation.

### 4.3. Evolution of the Group Gas

The global x-ray properties of groups are consistent with groups being scaled-down versions of clusters (Price et al. 1991; Henry et al. 1995; Mulchaey & Zabludoff 1998). But, the wide variations seen the abundance, abundance ratios and  $M_{Fe}/L_B$  in group gas argues strongly that the evolution of group gas is not simply a scaled down version of cluster evolution. In clusters the primary source of metals is thought to be from the early evolution of elliptical galaxies. Proto-elliptical galaxies



are thought to undergo a burst of star formation and subsequently lose roughly half of their original mass in winds driven by supernova explosions (David et al. 1994). Analysis of ASCA data indicate that these early winds are driven by type II SNe (Loewenstein & Mushotzky 1996). Later, as the progenitors of the type II events are not replenished, type I SNe continue to drive winds, albeit with a much diminished mass loss rate.

Winds blown from elliptical galaxies can reach speeds of  $\sim 1000$  km/s and for systems less massive than  $\sim 3 \times 10^{13} M_{\odot}$  the wind will not be bound to the system. Clusters, with masses  $\sim 10^{14} - 10^{15} M_{\odot}$ , can retain the enriched gas blown off by elliptical galaxies. But, because group masses show a range of  $\sim 10^{12} - 10^{13} M_{\odot}$  (Mulchaey et al. 1996) it is not surprising to see that groups may retain only some part of that enriched gas. This can also explain the difference in the  $\langle A_{\alpha} \rangle / \langle A_{Fe} \rangle$  ratio. If the early winds from ellipticals are lost by the groups then they also lose the material enriched primarily by type II SNe. Currently ellipticals are predicted to have mass loss rates of  $\sim 1.5 \times 10^{-11} M_{\odot} \text{ yr}^{-1} L_B$  (Faber & Gallagher 1976). This can produce about  $10^6 M_{\odot}$  of iron in  $10^{10}$  years for a typical group luminosity of  $2 \times 10^{11} L_B$  which could supply only 10% of the iron seen in groups today. Any winds from ellipticals are currently driven by type I SNe, and the abundance ratios in groups indicate that type I SNe play a larger role in enriching the group gas than in enriching cluster gas. However, the presence of  $\alpha$ -elements shows that groups have retained some of the type II SNe ejecta and this could provide a source of additional iron and raise the iron mass to the present day values of between  $10^7 - 10^8 M_{\odot}$ .

## 5. Baryonic fraction of the Ejected Material and the Intergalactic Medium

If, as we argue above, most of the enriched intra-group medium has been ejected then this indicates that groups can pollute the primordial gas in the intergalactic medium. Simulations show that during the early evolution of ellipticals they lose about half of their total mass as supernova induced winds (David et al. 1991). We can estimate the total fraction of baryons ejected from groups using the data in Mulchaey et al. (1996) and in Fukugita et al. (1998). If we assume that the galaxy mass has decreased by a factor of two due to winds and that this extra enriched gas has been ejected from the group, we find that  $\Omega_B \sim 0.008 h_{50}^{-1.5}$  where  $\Omega_B$  is the fraction that the baryons contribute to the critical density in an Einstein-de Sitter universe. This is less than the value that Fukugita et al. find for cool plasma in low surface density clouds outside of groups, clusters and galaxies. Converting the value of  $\Omega$  given by Fukugita et al. (1998) for the Lyman- $\alpha$  forest and the damped absorbers to  $H_0$  of 50 yields a value of 0.024. So, if groups do eject gas at early epochs, then they may contribute gas to the Lyman- $\alpha$  forest and can account for about 1/3 of the gas seen.

## 6. Conclusions

We have analyzed the x-ray data for seventeen groups of galaxies observed by ASCA. We have determined the global temperature and abundance for each of the groups. We have also determined the abundance of  $\alpha$ -elements for ten of the groups and investigated the abundance of O, S, Si, and Fe for several systems.

The global temperature of the groups are all  $\sim 1$  keV but the metal abundance can vary widely from  $<0.05 - 0.55$  solar. We find that the metal abundance in groups drops rapidly as the temperature drops. The best fit correlation shows that  $A \propto T(\text{keV})^{+2.5}$  and is in the opposite direction than the correlation found for clusters. The mass of metals per unit blue light also drops rapidly as the group temperature drops. We interpret this as evidence for winds in the early history of the group.

Further evidence for group-scale winds comes from fitting the abundances of the  $\alpha$ -elements and iron separately. We find that for cool groups ( $kT < 1.5$  keV) the  $\langle A_\alpha \rangle / \langle A_{Fe} \rangle$  ratio is  $\sim 1$  but for hotter groups it is  $\sim 2$ . This strongly suggests that, unlike clusters, groups lose most of the gas enriched by type II SNe during the early life of an elliptical galaxy. This has strong implications for the existence of a metal enriched intergalactic medium in the low redshift universe. Simple calculations indicate that most of the baryons have been ejected from groups and thus groups contribute to a putative metal rich intergalactic medium.

The spectral resolution of the ASCA SIS has provided unique insight into the evolution of groups of galaxies. However, future work will require better spatial resolution and sufficient spectral resolution to determine elemental abundances in a sample of groups: a project well suited to AXAF.

research at M.I.T. is supported in part by the AXAF Science Center as part of Smithsonian Astrophysical Observatory contract SVI-61010 under NASA Marshall Space Flight Center.

We would like to thank our referee for helpful comments which improved the paper. This research made use of the HEASARC, NED, and SkyView databases. Partial support for this project was provided by NASA grants NAG 5-3321, NAG 5-3529 and NAG 6-6143. DSD's

## REFERENCES

- Arnaud, M. Rothenflug, R., Bloulade, O., Vigroux, L. & Vangioni-Flam, E. 1992, AA, 254, 49
- Bahcall, N. A., Harris, D. E. & Rood, H. J. 1984, ApJ, L29
- Bauer, F. & Bregman J. N. 1997, ApJ, 457, 382
- Biermann, P., Kronberg, P.P. & Madore, B. F. 1982, ApJ, 256, L37
- Ciotti, L., D’Ercole, A., Pellegrini, S. & Renzini, A. 1991, ApJ, 376, 380
- David, L. P., Arnaud, K. A., Forman, W. & Jones, C. 1991, ApJ, 356, 32
- David, L. P., Forman, W. & Jones, C. 1991, ApJ, 356, 32
- David, L. P., Jones, C., Forman, W. & Daines, S. 1994 ApJ 445, 578
- Davis, D.S., Mushotzky, R.F., Mulchaey, J.S., Worrall, D., Birkinshaw, M. & Burstein, D. 1996, ApJ, 460, 601
- Dickey & Lockman 1990, Ann. Rev. Ast. Astr., 28, 215
- Dressler, A. 1980, ApJ 236, 351
- Faber, S. M. & Gallagher, J. S. 1976, ApJ, 204, 365
- Fukugita, M., Hogan, C. J. & Peebles, P. E. J. 1998, ApJ submitted
- Fukazawa, Y, Makishima, K., Matsushita, K., Yamasaki, N., Ohashi, T., Mushotzky, R. F., Sakima, Y., Tsusaka, Y., Yamashita, K. 1996, PASJ, 48, 395
- Gibson, B. K., Loewenstein, M. & Mushotzky, R. 1997 MNRAS, 290, 623
- Gnedin, O. Y. & Ostriker, J. P. 1997, ApJ, 474, 223
- Hatsukade, I. 1989, PhD Thesis, Osaka University
- Henry, J. P., Gioia, I. M., Huchra, J. P., Burg, R., McLean, B., Bohringer, H., Bower, R. G., Briel, U. G., Voges, W., MacGillivray, H., Cruddace, R. G. 1995, ApJ, 449, 422
- Hickson, P., Kindl, E. & Auman, J. R. 1989, ApJS, 70, 687
- Hwang, U. 1997 private communication
- Loewenstein, M. & Mushotzky, R. F. 1996, ApJ, 466, 695
- Madau, P. 1997 "The Hubble Deep Field", ed. M. Livio, S. M. Fall, & P. Madau, STScI Symposium Series
- Mulchaey, J. S., Davis, D. S., Mushotzky, R. F. & Burstein, D. 1993, ApJ, 404, L9
- Mulchaey, J. S., Davis, D. S., Mushotzky, R. F. & Burstein, D. 1996, ApJ, 456, 80
- Mulchaey, J. S., Davis, D. S. & Mushotzky, R. F. 1998, in prep
- Mushotzky, R. F., Loewenstein, M., Arnaud, K. A., Tamura, T., Fukazawa, Y., Matsushita, K., Kikuchi, K. & Hatsukade, I. 1996, ApJ, 466, 686

- Pildis, R. A., Bregman, J. N. & Evrard, A. E. 1995, *ApJ*, 443, 514
- Ponman, T. J., Bourner, P. D. J., Ebeling, H., & Bohringer, H. 1996, *MNRAS*, 283, 690
- Price, R., Burns, J. O., Duric, N. & Newberry, M. V. 1991, *AJ*, 102, 14
- Renzini, A., Ciotti, L., D’Ercole, A. & Pellegrini, S. 1993 *ApJ*, 419, 52
- Renzini, A. 1997, *ApJ*, 488, 35
- Scharf, C. A. & Mushotzky, R. F. 1997, *ApJ*, 485, L65
- White, R. E. III, *ApJ*, 367, 69
- Woosley, S. E. & Weaver, T. A. 1995, *ApJS*, 101, 181
- Wyse, R. F. G. 1998, *ApJL* in press
- Zabludoff, A. & Mulchaey, J. S. 1998, *ApJ*, 496, 39

Table 1: Basic Data for Poor Groups

Group	R.A. J2000	Dec. J2000	Velocity km s <sup>-1</sup>	$\sigma$ km s <sup>-1</sup>	L <sub>b</sub> 10 <sup>11</sup> M <sub>⊙</sub>
NGC 2300	07 32 20	+85 42 31	2074	251	1.1
NGC 2563	08 20 36	+21 04 00	4890 <sup>a</sup>	336	3.1
HCG 42	09 57 52	−19 23 56	3990	214 <sup>b</sup>	2.7
NGC 3258	10 28 54	−35 36 22	2852	176	6.7
HCG 51	11 22 21	+24 17 35	7740	240 <sup>b</sup>	3.7
HCG 57	11 35 17	+22 15 28	9120	269 <sup>b</sup>	5.1
NGC 4104	12 06 39	+28 10 18	8480	546 <sup>c</sup>	4.8
HCG 62	12 50 30	−08 55 59	4110	288 <sup>d</sup>	0.9
NGC 4325	12 23 07	+10 37 10	7558	265 <sup>a</sup>	2.4
NGC 5044	13 14 23	−16 32 04	2459	360	1.7
RGH 80	13 18 06	+33 27	11098	467	1.8
NGC 5129	13 24 10	+13 58 33	7096	208	4.5
MKW 9	15 32 29	+04 40 54	11253	336 <sup>c</sup>	7.7
NGC 6329	17 14 15	+43 41 04	8223 <sup>e</sup>	...	1.5
Pavo	20 18 12	−70 53 19	3815 <sup>f</sup>	169 <sup>f</sup>	4.7
HCG 92	22 35 58	+33 57 36	6450	389	4.2
Pegasus	23 20 32	+08 11 27	4197	780 <sup>d</sup>	15.6

<sup>a</sup>Zabludoff & Mulchaey 1997

<sup>b</sup>Hickson et al. 1992

<sup>c</sup>Beers et al. 1995

<sup>d</sup>Fadda et al. 1996

<sup>e</sup>Velocity from the RC3

<sup>f</sup>Bi-weight estimates

Table 2: Global X-ray Data for Poor Groups

Group	Temperature keV	Abundance Solar	$N_h/10^{20}$ atoms $\text{cm}^{-2}$	$N_h/10^{20}(\text{Gal})$ atoms $\text{cm}^{-2}$	$R_{\text{extract}}$ '	$\chi^2/\text{dof}$
NGC 2300	$0.88^{+0.04}_{-0.05}$	< 0.05	$4.25^a$	4.25	25	37/57
NGC 2563	$1.39^{+0.05}_{-0.06}$	$0.55^{+0.24}_{-0.17}$	$3.92^a$	3.92	20	356/248
HCG 42	$0.90^{+0.03}_{-0.02}$	$0.27^{+0.11}_{-0.07}$	$5.32^a$	5.32	8	91/78
NGC 3258	$1.85^{+0.23}_{-0.22}$	$0.28^{+0.21}_{-0.18}$	$6.48^a$	6.48	13	324/290
HCG 51	$1.24^{+0.04}_{-0.08}$	$0.41^{+0.06}_{-0.10}$	$7.96^{+3.10}_{-2.42}$	1.27	7	454/347
HCG 57	$1.15^{+0.21}_{-0.08}$	$0.14^{+0.26}_{-0.09}$	$1.82^a$	1.82	10	327/274
NGC 4104	$2.16^{+0.15}_{-0.18}$	$0.41^{+0.10}_{-0.09}$	$0.15^{+3.47}_{-0.15}$	1.69	12	463/459
HCG 62	$0.95^{+0.03}_{-0.03}$	$0.21^{+0.03}_{-0.04}$	$6.29^{+5.11}_{-2.50}$	2.69	23	454/419
NGC 4325	$1.05^{+0.04}_{-0.03}$	$0.44^{+0.15}_{-0.10}$	<9.40	2.23	10	223/196
NGC 5044	$1.00^{+0.02}_{-0.02}$	$0.24^{+0.03}_{-0.03}$	<1.3	5.03	30	225/130
RGH 80	$1.04^{+0.02}_{-0.05}$	$0.19^{+0.04}_{-0.04}$	$6.80^{+8.20}_{-6.50}$	1.03	10	348/319
NGC 5129	$0.87^{+0.02}_{-0.05}$	$0.14^{+0.05}_{-0.03}$	<15.7	1.77	12	299/271
MKW 9	$2.44^{+0.14}_{-0.11}$	$0.29^{+0.07}_{-0.06}$	<0.39	4.18	11	966/752
NGC 6329	$1.32^{+0.06}_{-0.06}$	$0.22^{+0.09}_{-0.05}$	$2.14^a$	2.14	13	306/285
Pavo	$0.82^{+0.04}_{-0.11}$	$0.09^{+0.36}_{-0.06}$	$0.06^{+19.70}_{-0.06}$	5.20	15	303/269
HCG 92 <sup>b</sup>	$0.76^{+0.05}_{-0.05}$	$0.11^{+0.10}_{-0.05}$	<7.42	8.00	4	157/160
Pegasus	$1.05^{+0.02}_{-0.03}$	$0.34^{+0.05}_{-0.04}$	$4.40^{+5.9}_{-3.35}$	5.03	23	480/474

<sup>a</sup>Parameter held constant during the fit

<sup>b</sup>Power law component was included in the fit

Table 3a: Global Spectral Fits with Variable Abundances

Group	Temperature	A <sub>α</sub>	A <sub>Fe</sub>	N <sub>h</sub> /10 <sup>20</sup>	χ <sup>2</sup> /dof
	keV	Solar	Solar	atoms cm <sup>-2</sup>	
NGC 4325	1.06 <sup>+0.02</sup> <sub>-0.06</sub>	0.31 <sup>+0.23</sup> <sub>-0.13</sub>	0.42 <sup>+0.14</sup> <sub>-0.09</sub>	<24.70	223/196
NGC 5129	0.87 <sup>+0.02</sup> <sub>-0.05</sub>	0.20 <sup>+0.26</sup> <sub>-0.14</sub>	0.16 <sup>+0.06</sup> <sub>-0.04</sub>	<24.1	297/271
NGC 4104	1.93 <sup>+0.13</sup> <sub>-0.19</sub>	0.80 <sup>+0.24</sup> <sub>-0.20</sub>	0.37 <sup>+0.11</sup> <sub>-0.12</sub>	0.17 <sup>+4.20</sup> <sub>-0.17</sub>	463/459
HCG 62	0.95 <sup>+0.03</sup> <sub>-0.03</sub>	0.23 <sup>+0.08</sup> <sub>-0.07</sub>	0.22 <sup>+0.04</sup> <sub>-0.04</sub>	5.96 <sup>+5.94</sup> <sub>-2.30</sub>	454/419
NGC 5044 <sup>1</sup>	1.01	0.30	0.36	6.5	...
RGH 80	1.02 <sup>+0.05</sup> <sub>-0.05</sub>	0.28 <sup>+0.16</sup> <sub>-0.08</sub>	0.20 <sup>+0.05</sup> <sub>-0.06</sub>	6.88 <sup>+9.40</sup> <sub>-5.63</sub>	335/317
MKW 9	2.18 <sup>+0.11</sup> <sub>-0.09</sub>	0.48 <sup>+0.15</sup> <sub>-0.13</sub>	0.24 <sup>+0.07</sup> <sub>-0.05</sub>	<7.47	954/748
Pavo	0.77 <sup>+0.07</sup> <sub>-0.05</sub>	0.10 <sup>+0.20</sup> <sub>-0.09</sub>	0.17 <sup>+0.88</sup> <sub>-0.04</sub>	<56.26	301/265
NGC 6329	1.32 <sup>+0.04</sup> <sub>-0.07</sub>	0.22 <sup>+0.20</sup> <sub>-0.13</sub>	0.24 <sup>+0.07</sup> <sub>-0.05</sub>	<10.7	298/281
Pegasus	1.04 <sup>+0.03</sup> <sub>-0.02</sub>	0.35 <sup>+0.41</sup> <sub>-0.09</sub>	0.33 <sup>+0.17</sup> <sub>-0.04</sub>	5.30 <sup>+7.9</sup> <sub>-5.3</sub>	480/474

<sup>1</sup>Fit was too poor to obtain errors for the parameters

Table 3b. Group Abundances for Individual Elements

Group	Radius (arcmin)	Temperature (keV)	$A_o$ (Solar)	$A_{Si}$ (Solar)	$A_S$ (Solar)	$A_{Fe}$ (Solar)	$N_h/10^{20}$ (atoms cm $^{-2}$ )	$\chi^2/\text{dof}$
NGC 4104	0-12	$1.79^{+0.30}_{-0.18}$	$1.87^{+3.55}_{-0.91}$	$0.75^{+0.46}_{-0.21}$	$0.43^{+0.26}_{-0.24}$	$0.31^{+0.21}_{-0.08}$	$6.59^{+6.08}_{-4.67}$	176/172
HCG 62	0-15	$1.00^{+0.02}_{-0.03}$	$<0.16$	$0.32^{+0.07}_{-0.08}$	$0.28^{+0.17}_{-0.15}$	$0.25 \pm 0.04$	$<12.6$	443/411
MKW 9	0-11	$2.23^{+0.22}_{-0.11}$	$<1.02$	$0.64^{+0.20}_{-0.16}$	$0.33^{+0.18}_{-0.20}$	$0.24^{+0.09}_{-0.06}$	$<7.98$	932/744
Pegasus	0-15	$1.06^{+0.03}_{-0.03}$	$0.52^{+1.07}_{-0.27}$	$0.40^{+0.24}_{-0.11}$	$0.46^{+0.34}_{-0.23}$	$0.34^{+0.21}_{-0.08}$	$<11.5$	494/472



TABLE 4  
MASS TO LIGHT RATIOS

Group	Gas Mass $10^{12} M_{\odot}$	Single Fits	$\alpha$ -elements Fit		O,Si,S,Fe Fits			
		$M_{Fe}/L_B$ ( $10^{-5} M_{\odot}/L_{\odot}$ )	$M_{\alpha}/L_B$ ( $10^{-3} M_{\odot}/L_{\odot}$ )	$M_{Fe}/L_B$ ( $10^{-5} M_{\odot}/L_{\odot}$ )	$M_O/L_B$ ( $10^{-3} M_{\odot}/L_{\odot}$ )	$M_{Si}/L_B$ ( $10^{-4} M_{\odot}/L_{\odot}$ )	$M_S/L_B$ ( $10^{-5} M_{\odot}/L_{\odot}$ )	$M_{Fe}/L_B$ ( $10^{-5} M_{\odot}/L_{\odot}$ )
NGC 2300	1.25	2.66	...	...	...	...	...	...
NGC 2563	2.00	16.6	...	...	...	...	...	...
HCG 42	0.24	1.12	...	...	...	...	...	...
NGC 3258	0.78	1.52	...	...	...	...	...	...
HCG 51	1.62	8.41	...	...	...	...	...	...
HCG 57	18.3	23.5	...	...	...	...	...	...
NGC 4104	6.58	26.3	11.7	24.4	21.8	3.65	9.55	19.9
HCG 62	4.19	45.8	11.4	47.9	<6.3	5.29	45.9	54.5
NGC 4325	2.66	22.8	3.66	21.8	...	...	...	...
NGC 5044	3.11	20.5	5.84	30.8	...	...	...	...
RGH 80	8.22	40.6	13.6	42.7	...	...	...	...
NGC 5129	6.26	9.11	2.96	10.4	...	...	...	...
MKW 9	0.35	0.62	0.23	0.52	0.40	10.4	24.5	0.52
NGC 6329	7.06	48.5	11.0	52.9	...	...	...	...
Pavo	0.40	0.36	0.09	0.68	...	...	...	...
HCG 92	0.16	0.02	...	...	...	...	...	...
Pegasus	8.35	8.53	1.99	8.27	2.37	18.2	3.99	8.52

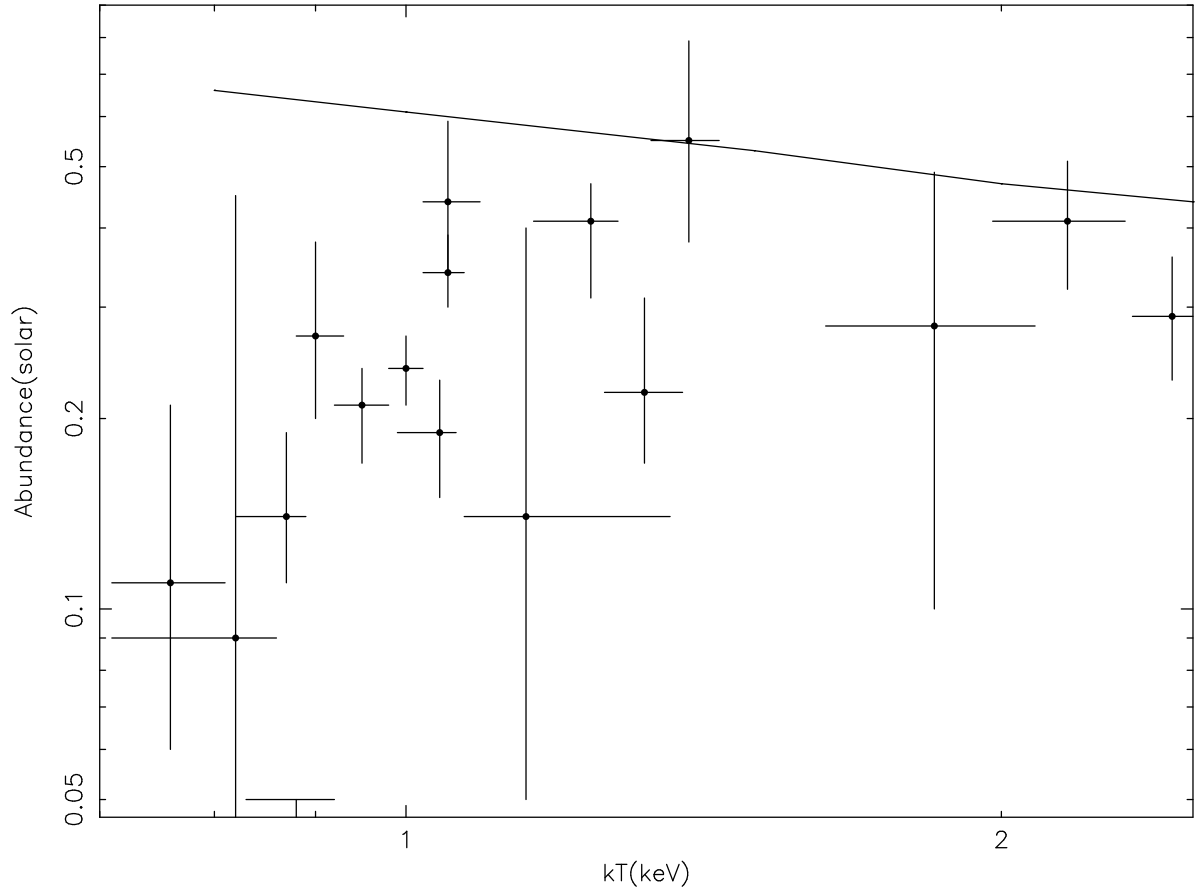


Fig. 1.— The abundance of the hot gas is plotted as a function of the gas temperature in keV. The error bars are the 90% confidence range for the quantities and the solid line shows the best fit for clusters of galaxies from Arnaud et al. (1992)

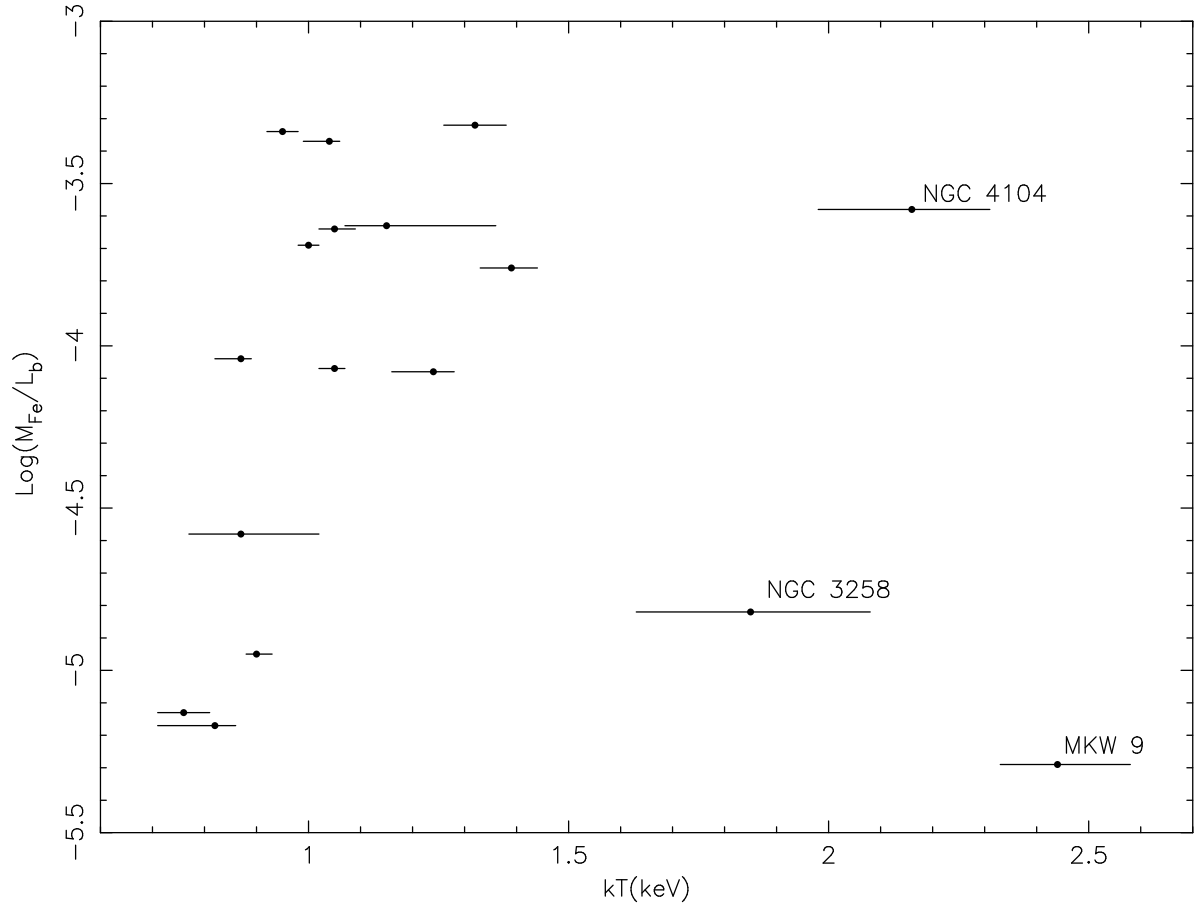


Fig. 2.— The iron mass to light ratio for the groups in this study is shown as a function of the diffuse gas temperature.

Table 1: Basic Data for Poor Groups

Group	R.A. J2000	Dec. J2000	Velocity km s <sup>-1</sup>	$\sigma$ km s <sup>-1</sup>	L <sub>b</sub> 10 <sup>11</sup> M <sub>⊙</sub>
NGC 2300	07 32 20	+85 42 31	2074	251	1.1
NGC 2563	08 20 36	+21 04 00	4890 <sup>a</sup>	336	3.1
HCG 42	09 57 52	-19 23 56	3990	214 <sup>b</sup>	2.7
NGC 3258	10 28 54	-35 36 22	2852	176	6.7
HCG 51	11 22 21	+24 17 35	7740	240 <sup>b</sup>	3.7
HCG 57	11 35 17	+22 15 28	9120	269 <sup>b</sup>	5.1
NGC 4104	12 06 39	+28 10 18	8480	546 <sup>c</sup>	4.8
HCG 62	12 50 30	-08 55 59	4110	288 <sup>d</sup>	0.9
NGC 4325	12 23 07	+10 37 10	7558	265 <sup>a</sup>	2.4
NGC 5044	13 14 23	-16 32 04	2459	360	1.7
RGH 80	13 18 06	+33 27	11098	467	1.8
NGC 5129	13 24 10	+13 58 33	7096	208	4.5
MKW 9	15 32 29	+04 40 54	11253	336 <sup>c</sup>	7.7
NGC 6329	17 14 15	+43 41 04	8223 <sup>e</sup>	...	1.5
Pavo	20 18 12	-70 53 19	3815 <sup>f</sup>	169 <sup>f</sup>	4.7
HCG 92	22 35 58	+33 57 36	6450	389	4.2
Pegasus	23 20 32	+08 11 27	4197	780 <sup>d</sup>	15.6

<sup>a</sup>Zabludoff & Mulchaey 1997<sup>b</sup>Hickson et al. 1992<sup>c</sup>Beers et al. 1995<sup>d</sup>Fadda et al. 1996<sup>e</sup>Velocity from the RC3<sup>f</sup>Bi-weight estimates

Table 2: Global X-ray Data for Poor Groups

Group	Temperature keV	Abundance Solar	$N_h/10^{20}$ atoms $\text{cm}^{-2}$	$N_h/10^{20}(\text{Gal})$ atoms $\text{cm}^{-2}$	$R_{\text{extract}}$ /	$\chi^2/\text{dof}$
NGC 2300	$0.88^{+0.04}_{-0.05}$	$< 0.05$	$4.25^a$	4.25	25	37/57
NGC 2563	$1.39^{+0.05}_{-0.06}$	$0.55^{+0.24}_{-0.17}$	$3.92^a$	3.92	20	356/248
HCG 42	$0.90^{+0.03}_{-0.02}$	$0.27^{+0.11}_{-0.07}$	$5.32^a$	5.32	8	91/78
NGC 3258	$1.85^{+0.23}_{-0.22}$	$0.28^{+0.21}_{-0.18}$	$6.48^a$	6.48	13	324/290
HCG 51	$1.24^{+0.04}_{-0.08}$	$0.41^{+0.06}_{-0.10}$	$7.96^{+3.10}_{-2.42}$	1.27	7	454/347
HCG 57	$1.15^{+0.21}_{-0.08}$	$0.14^{+0.26}_{-0.09}$	$1.82^a$	1.82	10	327/274
NGC 4104	$2.16^{+0.15}_{-0.18}$	$0.41^{+0.10}_{-0.09}$	$0.15^{+3.47}_{-0.15}$	1.69	12	463/459
HCG 62	$0.95^{+0.03}_{-0.03}$	$0.21^{+0.03}_{-0.04}$	$6.29^{+5.11}_{-2.50}$	2.69	23	454/419
NGC 4325	$1.05^{+0.04}_{-0.03}$	$0.44^{+0.15}_{-0.10}$	$< 9.40$	2.23	10	223/196
NGC 5044	$1.00^{+0.02}_{-0.02}$	$0.24^{+0.03}_{-0.03}$	$< 1.3$	5.03	30	225/130
RGH 80	$1.04^{+0.02}_{-0.05}$	$0.19^{+0.04}_{-0.04}$	$6.80^{+8.20}_{-6.50}$	1.03	10	348/319
NGC 5129	$0.87^{+0.02}_{-0.05}$	$0.14^{+0.05}_{-0.03}$	$< 15.7$	1.77	12	299/271
MKW 9	$2.44^{+0.14}_{-0.11}$	$0.29^{+0.07}_{-0.06}$	$< 0.39$	4.18	11	966/752
NGC 6329	$1.32^{+0.06}_{-0.06}$	$0.22^{+0.09}_{-0.05}$	$2.14^a$	2.14	13	306/285
Pavo	$0.82^{+0.04}_{-0.11}$	$0.09^{+0.36}_{-0.06}$	$0.06^{+19.70}_{-0.06}$	5.20	15	303/269
HCG 92 <sup>b</sup>	$0.76^{+0.05}_{-0.05}$	$0.11^{+0.10}_{-0.05}$	$< 7.42$	8.00	4	157/160
Pegasus	$1.05^{+0.02}_{-0.03}$	$0.34^{+0.05}_{-0.04}$	$4.40^{+5.9}_{-3.35}$	5.03	23	480/474

<sup>a</sup>Parameter held constant during the fit<sup>b</sup>Power law component was included in the fit

Table 3a: Global Spectral Fits with Variable Abundances

Group	Temperature	A <sub>α</sub>	A <sub>Fe</sub>	N <sub>h</sub> /10 <sup>20</sup>	χ <sup>2</sup> /dof
	keV	Solar	Solar	atoms cm <sup>-2</sup>	
NGC 4325	1.06 <sup>+0.02</sup> <sub>-0.06</sub>	0.31 <sup>+0.23</sup> <sub>-0.13</sub>	0.42 <sup>+0.14</sup> <sub>-0.09</sub>	<24.70	223/196
NGC 5129	0.87 <sup>+0.02</sup> <sub>-0.05</sub>	0.20 <sup>+0.26</sup> <sub>-0.14</sub>	0.16 <sup>+0.06</sup> <sub>-0.04</sub>	<24.1	297/271
NGC 4104	1.93 <sup>+0.13</sup> <sub>-0.19</sub>	0.80 <sup>+0.24</sup> <sub>-0.20</sub>	0.37 <sup>+0.11</sup> <sub>-0.12</sub>	0.17 <sup>+4.20</sup> <sub>-0.17</sub>	463/459
HCG 62	0.95 <sup>+0.03</sup> <sub>-0.03</sub>	0.23 <sup>+0.08</sup> <sub>-0.07</sub>	0.22 <sup>+0.04</sup> <sub>-0.04</sub>	5.96 <sup>+5.94</sup> <sub>-2.30</sub>	454/419
NGC 5044 <sup>1</sup>	1.01	0.30	0.36	6.5	...
RGH 80	1.02 <sup>+0.05</sup> <sub>-0.05</sub>	0.28 <sup>+0.16</sup> <sub>-0.08</sub>	0.20 <sup>+0.05</sup> <sub>-0.06</sub>	6.88 <sup>+9.40</sup> <sub>-5.63</sub>	335/317
MKW 9	2.18 <sup>+0.11</sup> <sub>-0.09</sub>	0.48 <sup>+0.15</sup> <sub>-0.13</sub>	0.24 <sup>+0.07</sup> <sub>-0.05</sub>	<7.47	954/748
Pavo	0.77 <sup>+0.07</sup> <sub>-0.05</sub>	0.10 <sup>+0.20</sup> <sub>-0.09</sub>	0.17 <sup>+0.88</sup> <sub>-0.04</sub>	<56.26	301/265
NGC 6329	1.32 <sup>+0.04</sup> <sub>-0.07</sub>	0.22 <sup>+0.20</sup> <sub>-0.13</sub>	0.24 <sup>+0.07</sup> <sub>-0.05</sub>	<10.7	298/281
Pegasus	1.04 <sup>+0.03</sup> <sub>-0.02</sub>	0.35 <sup>+0.41</sup> <sub>-0.09</sub>	0.33 <sup>+0.17</sup> <sub>-0.04</sub>	5.30 <sup>+7.9</sup> <sub>-5.3</sub>	480/474

<sup>1</sup>Fit was too poor to obtain errors for the parameters

TABLE 3B  
GROUP ABUNDANCES FOR INDIVIDUAL ELEMENTS

Group	Radius (arcmin)	Temperature (keV)	$A_o$ (Solar)	$A_{Si}$ (Solar)	$A_S$ (Solar)	$A_{Fe}$ (Solar)	$N_h/10^{20}$ (atoms cm $^{-2}$ )	$\chi^2/\text{dof}$
NGC 4104	0-12	$1.79^{+0.30}_{-0.18}$	$1.87^{+3.55}_{-0.91}$	$0.75^{+0.46}_{-0.21}$	$0.43^{+0.26}_{-0.24}$	$0.31^{+0.21}_{-0.08}$	$6.59^{+6.08}_{-4.67}$	176/172
HCG 62	0-15	$1.00^{+0.02}_{-0.03}$	<0.16	$0.32^{+0.07}_{-0.08}$	$0.28^{+0.17}_{-0.15}$	$0.25 \pm 0.04$	<12.6	443/411
MKW 9	0-11	$2.23^{+0.22}_{-0.11}$	<1.02	$0.64^{+0.20}_{-0.16}$	$0.33^{+0.18}_{-0.20}$	$0.24^{+0.09}_{-0.06}$	<7.98	932/744
Pegasus	0-15	$1.06^{+0.03}_{-0.03}$	$0.52^{+1.07}_{-0.27}$	$0.40^{+0.24}_{-0.11}$	$0.46^{+0.34}_{-0.23}$	$0.34^{+0.21}_{-0.08}$	<11.5	494/472